AD-A111 770 JOHNS HOPKINS UNIV LAUREL MD APPLIED PHYSICS LAB F/G 20/4
APPROXIMATE METHOD FOR PREDICTING SUPERSONIC NORMAL FORCE COEFF--ETC(U)
MAY 81 E F LUCERO

UNCLASSIFIED

NL

END
DATE FILMED
4-82
DTIC

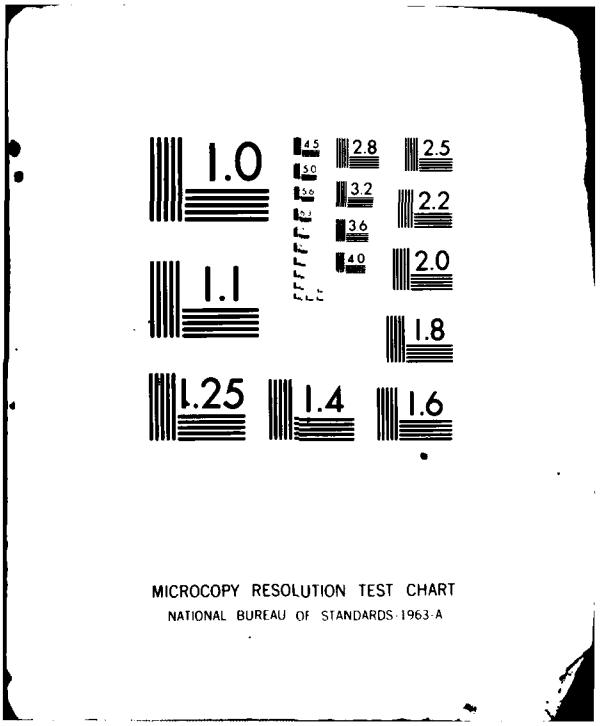
1.0
1.1
1.25
1.4
1.6
1.8
2.0
2.2
2.5
2.8
3.2
3.6
4.0
4.5
5.0
5.6
6.3
7.1
MICROCOPY RESOLUTION TEST CHART
NATIONAL BUREAU OF STANDARDS-1963-A

APPROXIMATE METHOD FOR PREDICTING SUPERSONIC NORMAL FORCE COEFFICIENT OF VERY-LOW-ASPECT-RATIO LIFTING SURFACES

E. F. Lucero
The Johns Hopkins University/Applied Physics Laboratory
Laurel, Maryland 20810

14 May 81

ABSTRACT

A simple, empirical method has been developed for predicting at supersonic speeds the normal force coefficient, C_N, (including carryover) of very-low-aspect ratio lifting surfaces mounted on bodies of revolution. Predicted values of C_N using this method are shown to be in good agreement with test data obtained on both thick and thin surfaces, at Mach numbers from about 2.5 to 7.7 and angles of attack to 24°.

SYMBOLS AND NOMENCLATURE

A_c, A_I, A_o	cross-sectional areas of the forebodies of the inlets, the inlets, and the freestream tube captured by the inlets of ramjet missiles, respectively	in^2
A.R.	aspect ratio = b^2/S_E or b^2/S_W	
b/2	exposed semi-span of a lifting surface mounted on a body of revolution	in
C_{D_c}	cross-flow drag coefficient	
C_N	normal force coefficient, normal force/qS	
C_{N_α}	$\partial C_N/\partial\alpha$	per rad
$\Delta C_{N_E}, \Delta C_{N_W}$	$C_{N_{BE}} - C_{N_B}$; $C_{N_{BW}} - C_{N_B}$ at $\phi = 0°$	
C_r	root chord	in

Supported by NAVSEA 62R

d	reference diameter; diameter of body on which lifting surfaces are mounted	in
E	complete elliptic integral of second kind with modulus $(1 - \beta^2 \cot^2 \Lambda)^{\frac{1}{2}}$	
K_B, K_W	Morikawa's interference factors	
M	Mach number	
q	dynamic pressure	lbs/in^2
S	reference area, $\pi d^2/4$	in^2
S_E, S_W	total planform area of housings (wings)	in^2
t	average thickness of lifting surface	in
X	body station; X = 0 at nose tip of body	in
$X_{c.p.}$	center-of-pressure location	in
α	angle of attack; angle between the velocity vector and the longitudinal axis of the body	deg
β	$\sqrt{M^2 - 1}$	
γ	ratio of specific heats; $\gamma = 1.4$ used herein	
Λ	leading edge sweep angle for delta wings	deg
ϕ	aerodynamic roll angle; at $\phi = 0°$ tne lifting surfaces are normal to the plane of α	deg

Subscripts

B	body alone
BE	body-housing combination
BW	body-wing combination
E	housing
I	refers to inlet forebody and internal lift as in ΔC_{N_I}
W	wing

INTRODUCTION

The requirement for compactness in U. S. Navy missile designs results frequently in configurations which incorporate thick lifting surfaces of very-low-aspect ratio. These surfaces are invariably thick, e.g., Figures 1 and 2, because they are used to house electronics and hydraulics or serve as ducts, as in the case of side-mounted inlets on ramjet missiles. Current requirements on missile speed have increased to regions where guidance for making aerodynamic estimates for these surfaces is not available, either from theory or experiment.

Empirical estimation of the normal force coefficient, C_N, and center-of-pressure location, $X_{c.p.}$, for these surfaces is difficult because the shapes are usually unique for each new missile design and, therefore, the limited test data available are invariably for shapes that are quite different from the proposed shape in a new missile design. Existing empirical methods[1] have been derived for a specific class of surfaces and apply to the lower end of the Mach number range of interest in this presentation.

Simple theoretical methods that have been used (with limited success) do not take into account the effects of Mach number. Those that do, are not applicable at the very low values of aspect ratio inherent to these types of surfaces. These concerns have been expressed for some time.[2,3]

A need exists, therefore, for either an empirical data base for a more general class of low-aspect-ratio lifting surfaces or a simple predictive method that is adequate in preliminary design for predicting C_N and $X_{c.p.}$ of this class of surfaces in speed ranges from moderate supersonic to hypersonic.

A simple, empirical predictive method for estimating C_N for very-low-aspect ratio surfaces is presented herein. It is shown to provide estimates of C_N that are adequate for preliminary design for a variety of thicknesses and shapes and a wide range of Mach numbers ($M \approx 2.5$ to 7.7) and angles of attack (α to 24°).

OBJECTIVE

The objective of this study was to determine a simple method for estimating in preliminary design the aerodynamic normal force coefficient of very-low-aspect ratio lifting surfaces (and body-wing combinations) at moderate supersonic to hypersonic speeds and to moderate angles-of-attack.

METHODOLOGY

A. BACKGROUND

The method presented herein for predicting C_N of very-low-aspect-ratio lifting surfaces evolved from observations of the experimental lifting characteristics of thick surfaces such as those depicted by the housings on the wind tunnel model shown in Figure 1. This model is representative of an Integral Rocket-Ramjet (IRR) missile. It was tested by APL/JHU in order to compile aerodynamic design information for components of this class of configurations since empirical methods for predicting C_N and $X_{c.p.}$ for this type of configuration and combinations of components were not available. Hart's empirical curves[1] had been shown to provide good predictions for low-aspect-ratio surfaces at $M \lesssim 3.0$, but these curves had been derived mostly for wings that were primarily thin surfaces. The applicability of this method to thick surfaces and to higher Mach numbers was therefore not known.

Simple theoretical methods that account for the Mach number variation of ΔC_{N_W} noted from test data are not applicable at the very-low-aspect ratios of interest herein; those derived for aspect ratios approaching zero do not account for the Mach number effects. This is demonstrated in Figure 3 wherein the test values of ΔC_{N_W} of the IRR E_1 housings (ΔC_{N_E} minus internal momentum) are compared with two simple theoretical methods, viz: modified Newtonian theory,[4] plus wing-body carryover, i.e.,

$$\Delta C_{N_W} = \frac{\gamma + 3}{\gamma + 1}\left(1 - \frac{2}{\gamma + 3}\,\frac{1}{M^2}\right)\left(K_W + K_B\right)\frac{S_E}{S}\sin^2\alpha \qquad (1)$$

and slender wing theory[5] plus cross flow as recommended by Flax and Lawrence,[3] i.e.,

$$\Delta C_{N_W} = \left[\frac{\pi\ A.R.}{2 \times 57.3}\,\alpha + C_{D_c}\sin^2\alpha\right]\left(K_W + K_B\right)\frac{S_E}{S} \qquad (2)$$

The value of $C_{D_c} = 1.0$ was used in these calculations following the recommendation of Flax and Lawrence for the case of rounded tips. This number, however, could be something other than 1.0 according to Hoerner.[6] The Morikawa carryover factors[7] were used in Equations 1 and 2, and are used throughout this analysis.

B. APPROACH

Test data obtained on both thick and thin wings in various APL/JHU aerodynamic research and exploratory development programs were the primary source of data for the development of the empirical method presented herein. Selected

NASA data were also used. Sketches of the housing and wing configurations used in the analysis are given in Figures 4, 5, and 6; the sources for the test data[8-16] are noted in the figures for each configuration.

In all cases, the wing (or housing) data were obtained from tests conducted with cruciform wing-body and with body alone configurations. The wing-body was roll oriented at $\phi = 0°$, i.e., one pair of wings in the angle-of-attack plane. The test data then are derived from $\Delta C_{N_W} = C_{N_{BW}} - C_{N_B}$ and thus wing-body carryover is included in the wing lift.

The general approach in deriving and evaluating the present method using the test data discussed above, is:

1. Values of $\beta C_{N_{\alpha_W}}$ were extracted from test data obtained on the wing configurations sketched in Figures 4, 5, and 6.

2. Correlation curves of $\beta C_{N_{\alpha_W}}$ were deduced from the test values as follows: $\beta C_{N_{\alpha_W}} = F(\beta \text{ A.R.})$ for rectangular wings,

$\beta C_{N_{\alpha_W}} = F(\beta \cot\Lambda)$ for delta wings, and

$\beta C_{N_{\alpha_W}} =$ constant for thick wings.

A comparison of the derived curves with appropriate linear and slender wing theories is given.

3. These empirically derived curves were then used to calculate the values of ΔC_{N_W} for the 29 Mach number-configurational combinations used in the analysis. Comparisons with test data are given to demonstrate the adequacy of the present method.

RESULTS

A. PROCEDURE FOR EXTRACTING $\beta C_{N_{\alpha_W}}$ FROM TEST DATA

Values of $\beta C_{N_{\alpha_W}}$ that provide a good representation of the test data in the range of angle of attack tested were derived by first linearizing ΔC_{N_W} vs α as demonstrated in Figure 7 and then extracting $C_{N_{\alpha_W}}$ from the linearized values

of ΔC_{N_W} as follows:

$$C_{N_{\alpha_W}} = \frac{(57.3)\ (S/S_W)}{K_W + K_B} \quad \frac{\Delta C_{N_W}}{\alpha} \text{ , per rad.} \tag{3}$$

where $\Delta C_{N_W} = C_{N_{BW}} - C_{N_B}$ and this includes mutual body-wing carryover. The carryover factors K_W and K_B were obtained from Morikawa's charts, Reference 7; Morikawa's values of K_W for rectangular wings were used for the configurations that are nearly rectangular. In the linearization of ΔC_{N_W} vs α, more emphasis was given to obtaining a representation of ΔC_{N_W} at the moderate to higher values of α than at the lower values according to the objective of this investigation.

The E_1, E_2, and E_3 configurations of Figure 4 have flow through the inlet-duct system and thus ΔC_{N_E} for these configurations include internal lift. The lift attributed to the inlet forebody and internal momentum was subtracted from the total lift of these housings in order to obtain ΔC_{N_W} since we are only interested in the external lift. Thus, for these configurations,

$$\Delta C_{N_W} = \Delta C_{N_E} - \Delta C_{N_I} = \Delta C_{N_E} - 2\left(\frac{A_o}{A_I}\ \frac{A_I}{S} + \frac{A_c}{S}\right) \sin\alpha \tag{4}$$

A value of $A_o/A_I = 1.0$ was used in these calculations since the internal shock was not expelled for the cases considered. A_I and A_c are the combined cross sectional areas of the inlets and inlet forebodies, respectively.

Finally, the derived slopes were expressed in the usual functional forms found in design charts, i.e.,

$$\beta\ C_{N_{\alpha_W}} = F\ (\beta\ A.R.)$$

for rectangular wings, and

$$\beta\ C_{N_{\alpha_W}} = F\ (\beta \cot \Lambda\ )$$

for delta wings.

B. CORRELATION CURVES OF $\beta C_{N_{\alpha_W}}$

1. Nearly-Rectangular Wings

The "best fit" values of $\beta C_{N_{\alpha_W}}$ deduced from the test data on the nearly-rectangular housings and wings of Figures 4 and 5 are plotted in Figure 8 as a function of $1/\beta$ A.R. For comparison, the values of $\beta C_{N_{\alpha_W}}$ predicted from linear and slender wing theories, Reference 5, for rectangular wings, are also shown in Figure 8, i.e.,

$$\beta C_{N_{\alpha_W}} = 4 \left(1 - \frac{1}{2 \beta \text{ A.R.}}\right) \qquad \beta \text{ A.R.} > 1$$

$$\beta C_{N_{\alpha_W}} = \frac{4}{\pi} \left[\left(2 - \frac{1}{\beta \text{ A.R.}}\right) \sin^{-1} \beta \text{ A.R.} + (\beta \text{ A.R.} - 2) \cosh^{-1} \frac{1}{\beta \text{ A.R.}} + \left(1 + \frac{1}{\beta \text{ A.R.}}\right) \sqrt{1 - (\beta \text{ A.R.})^2}\right] \qquad \frac{1}{2} < \beta \text{ A.R.} < 1 \tag{5}$$

and,

$$\beta C_{N_{\alpha_W}} = \frac{\pi}{2} (\beta \text{ A.R.}) \qquad \beta \text{ A.R.} < 1/2 \text{ (Slender Wing)}$$

It is seen, from Figure 8, that the difference between experiment and theory (given by these simple methods) is very large for β A.R. $\gtrsim 0.67$ $[(1/\beta \text{ A.R.}) \approx 1.5]$.

Note that the theoretical values of C_{N_α} are lift curve slopes at $\alpha = 0°$ whereas the test values are the mean values of C_N/α obtained from the full range of α tested. For the test cases where C_N was linear with α ($M \gtrsim 3.0$), these two values should be the same. These theoretical methods are usually recommended in various handbooks and textbooks because of their success in predicting $C_{N_{\alpha_W}}$ at low values of α. Their success has been demonstrated by several investigators at the low values of α and at low supersonic Mach numbers. The inadequacy of these theoretical methods for predicting ΔC_{N_W}

without adding a non-linear term, such as cross-flow lift, was demonstrated by Flax and Lawrence[3] in 1951. Cross-flow lift for wings is a concept, taken from cross-flow lift on cylinders, which attempts to account for the vortex lift. The cross-flow drag value used in determining cross-flow lift is basically an experimental value obtained for a limited class of wings.[3,6] More recent approaches use the concept of leading-edge and side-edge suction[17,18] to account for non-linear lift. As far as can be established from the literature this approach is not applicable to the wing geometries of interest in this study.

Returning to the discussion of Figure 8, it is noted that the test values of $\beta C_{N_{\alpha_W}}$ for thick housings is generally lower than those for the "thin" wings. A separate R.M.S. curve for the thin wings demonstrates this. The value of $\beta C_{N_{\alpha_W}} = 4/3$ marked on the ordinate of Figure 8 will be shown later to provide a reasonable agreement with the majority of test values of ΔC_{N_W} for the thick wings used in this study, 12 Mach number-configurational combinations. The solid points shown in Figure 8 are for test cases where $M \lesssim 3.0$. In this region ΔC_{N_W} is very non-linear with α at low values of α. For these cases, it will be shown later that Hart's empirical method[1] provides good predictions at the lower values of α and for some cases at all values of α tested.

2. Thin Delta Wings

A similar correlation plot of $\beta C_{N_{\alpha_W}}$ for the test data for delta wings is given in Figure 9 and is compared with linear theory for these wings. In this case $\beta C_{N_{\alpha_W}}$ is given as a function of $\beta \cot \Lambda$ and plotted vs. $1/\beta \cot \Lambda$. The disagreement with linear theory is obvious. Note specifically that the test values of $\beta C_{N_{\alpha_W}}$ do not tend to 4 at $\beta \cot \Lambda = 1$ as predicted by linear theory but rather they tend to 4 at $\beta \cot \Lambda = \infty$ which is in agreement with predictions for rectangular wings.

3. Combined Correlation Curve for Very-Low-Aspect-Ratio Wings

A comparison of the R.M.S. curve of $\beta C_{N_{\alpha_W}} = F(1/\beta \text{ A.R.})$ for <u>thin</u> nearly-rectangular wings (Figure 8) with the R.M.S. curve of $\beta C_{N_{\alpha_W}} = F(1/\beta \cot \Lambda)$ for thin delta wings (Figure 9) shows that the two curves are essentially the same. Thus, one single curve is proposed for predicting $\beta C_{N_{\alpha_W}}$, for both thin rectangular (or nearly rectangular) and for delta wings. The curve has the same functional form for $\beta C_{N_{\alpha_W}}$ as shown in Figure 10. For

the thick wings, $\beta C_{N_{\alpha_W}} = 4/3$ is proposed for $(1/\beta \text{ A.R.}) \gtrsim 1.5$. Data were not found for thick surfaces for the region $(1/\beta \text{ A.R.}) \lesssim 1.5$ to determine the trend of $\beta C_{N_{\alpha_W}}$ for this region. The effect of wing thickness for ratios, t/d, between 0.2 and 0.1 also is not known; the thick wings used in the analyses had $t/d \geq 0.2$; the average "thickness" for the thin wings used was $t/d \lesssim 0.1$.

In summary, the correlation curves of Figure 10 are proposed as a simple empirical method for obtaining $\beta C_{N_{\alpha_W}}$ for very-low-aspect ratio wings. Since in practice these surfaces are usually mounted on a body of revolution the mutual body-wing interference should also be accounted for. Morikawa's factors are recommended for accounting for this interference mainly because they were used in deriving $\beta C_{N_{\alpha_W}}$ from test data. The adequacy of the proposed method for providing good engineering estimates of $\Delta C_{N_W} = C_{N_{BW}} - C_{N_B}$ at $M \gtrsim 2.5$ and α to about 24° is demonstrated in the next section.

C. COMPARISON OF TEST VALUES OF ΔC_{N_W} WITH EMPIRICAL PREDICTIONS USING THE PRESENT METHOD

The predicted values of ΔC_{N_W} are derived from the empirical curves of Figure 10 as follows:

$$\Delta C_{N_W} = \frac{\beta C_{N_{\alpha_W}}}{57.3\ \beta} (K_W + K_B) \frac{S_W}{S} \alpha \qquad (6)$$

where $\beta C_{N_{\alpha_W}}$ is per radian and α is in degrees. These values are compared in Figures 11 to 22 with the test data obtained from $C_{N_{BW}} - C_{N_B}$ for the 29 Mach number-configurational combinations used in the analysis. Calculated values of ΔC_{N_W} using Hart's method[1] are also shown, for the cases where this method is applicable, to demonstrate the adequacy of this method.

1. Thick Wings

Calculated values of ΔC_{N_W} using the present method, given by Figure 10 and Equation 6, are compared with test data from the thick housings in Figures 11 through 15. Values of ΔC_N obtained from Hart's empirical correlation curves[1] are also shown. The comparisons show, in general, that the

present method with $\beta C_{N_{\alpha_W}} = 4/3$ gives a good to excellent representation of the test values of ΔC_N to $\alpha = 24°$, $M \gtrsim 2.5$, for the five housing configurations of Figure 4. The predictions of the present method are especially good at $M \gtrsim 3.0$ where ΔC_{N_W} is nearly linear with α.

At $M \lesssim 3.0$, the data are very non-linear with α at low angles-of-attack and Hart's method gives a better prediction than the present method, see Figures 11 and 14. At the higher Mach numbers the present method provides a better prediction.

2. Thin Nearly-Rectangular Wings

The results of the evaluation of the present method for thin nearly-rectangular wings are given in Figures 16 through 19. The test data are for the configurations of Figure 5. The comparisons again show that the present method provides good predictions. Hart's method also gives good predictions in the region of applicability of his method, β A.R. $\lesssim 0.8$, but this method is not better than the present method.

3. Thin, Delta Wings

The present method provides excellent predictions for the test data for the delta wings of Figure 6, Figures 20, 21 and 22. Hart's method was not derived for delta wings and thus a comparison with this method is not made for these wings.

CONCLUSIONS

An empirical method is derived herein for estimating the normal force coefficient (plus wing-body carryover), ΔC_{N_W}, of nearly-rectangular thick and thin wings, and of thin delta wings, of very-low-aspect ratio. The method, in combination with Morikawa's interference factors, gives good predictions in the range of Mach numbers from 2.5 to 7.7 and angles of attack to 24°. For near-rectangular wings at $M \lesssim 3.0$, Hart's empirical correlation curves of Reference 1 are recommended for estimating ΔC_{N_W}.

REFERENCES

1. H. H. Hart, "An Aerodynamic Study of Very-Low-Aspect-Ratio, Nearly Rectangular Lifting Surfaces at Supersonic Speeds, APL/JHU CM-931, February 1958.

2. W. Hatalsky and P. H. Jackson, Jr., "Correlation of Theory and Experiment in the Supersonic Interference of Very Low Aspect Ratio Wings," Appendix II, Unclassified. Minutes of the Thirty-Sixth Regular Meeting, Bumblebee Aerodynamics Panel, June 1957, APL/JHU TG 14-33, August 1957, Confidential.

3. A. H. Flax and H. R. Lawrence, "The Aerodynamics of Low-Aspect-Ratio Wings and Wing-Body Combinations," Cornell Aeronautical Laboratory Report CAL-37, September 1951.

4. Robert Earl Oliver, An Experimental Investigation of Flow About Simple Blunt Bodies at a Nominal Mach Number of 5.8, Journal of the Aeronautical Sciences, February 1956.

5. Donovan and Lawrence, Editors, Aerodynamic Components of Aircraft at High Speeds, Volume VII, High Speed Aerodynamics and Jet Propulsion, Princeton University Press, 1957, Section A.14.

6. Hoerner and Borst, Fluid Dynamic Lift, page 17-7, published by Mrs. Liselotte A. Hoerner, 1975.

7. George Morikawa, "Supersonic Wing-Body Lift," Journal of the Aeronautical Sciences, Vol. 18, No. 4, April 1951.

8. E. F. Lucero, "Longitudinal Aerodynamics of the Configurational Components of the Integral Rocket-Ramjet (IRR) Configurations at Mach Numbers 2.0 to 4.5 and Angles of Attack to 24°," APL/JHU BFD-1-79-016, 25 September 1979.

9. General Dynamics/Convair High Speed Wind Tunnel Test Report HST 258-0, 3-5 May 1968.

10. General Dynamics/Convair High Speed Wind Tunnel Test Report HST 259-0, March 1968.

11. General Dynamics/Convair High Speed Wind Tunnel Test Report HST TR-009-0, July 1979.

12. E. F. Lucero, "Hypersonic Configuration Study, Part II: Body-Dorsal Configurations," APL/JHU BBA-2-71-021, 6 December 1971.

13. M. Leroy Spearman and Charles D. Trescott, Jr., "Effects of Wing Planform on the Static Aerodynamics of a Cruciform Wing-Body Missile for Mach Numbers up to 4.63," NASA TMX-1839, July 1969.

14. R. J. Vendemia, Jr., and M. P. Guthrie, "Effects of Variation of Lifting Surfaces' Leading and Trailing Edge Locations on Aerodynamic Normal Force, Pitching Moment, and Tail Characteristics of a Standardized Medium Range Type Missile at M = 2.5," APL/JHU BBA-SM-007-64, 8 May 1964.

15. APL/Navy Standard Missile Test Data Package: von Karman Gas Dynamics Facility, AEDC, U. S. Air Force, Tunnel A; Project No. V41A-N2A, Test Period: March 15-23, April 1-5, May 13-25, 1977.

16. General Dynamics/Convair High Speed Wind Tunnel Test Report HST-TAR-180-0, May 1966.

17. Edward C. Polhamus, "Predictions of Vortex-Lift Characteristics by a Leading-Edge Suction Analogy," Journal of Aircraft, Vol. 8, No. 4, April 1971.

18. John E. Lamar, "Prediction of Vortex Flow Characteristics of Wings at Subsonic and Supersonic Speeds," Journal of Aircraft, Vol. 13, No. 7, July 1976.

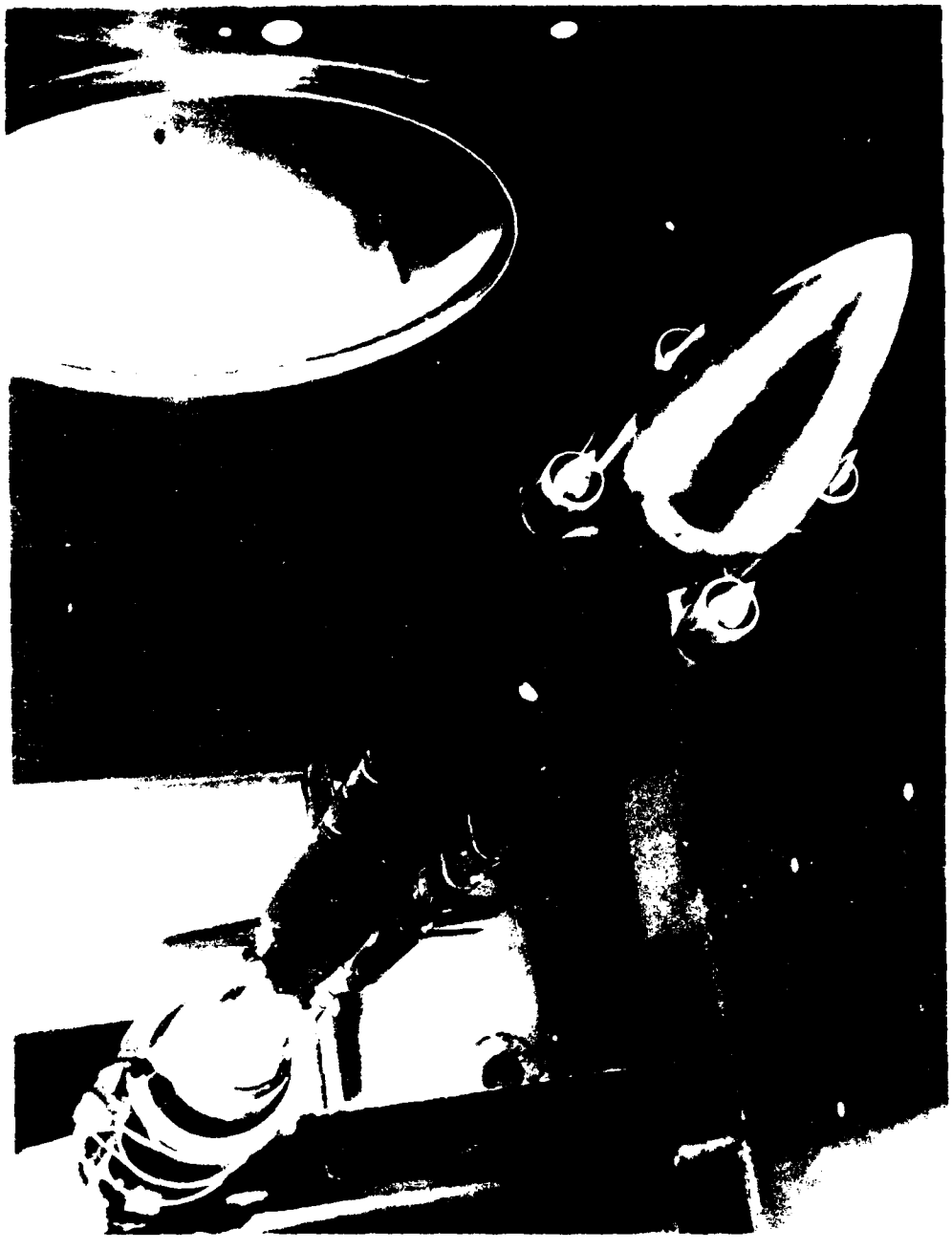

Fig. 1 Photo showing one type of very-low-aspect ratio, thick housings (with flow through) used in analysis.

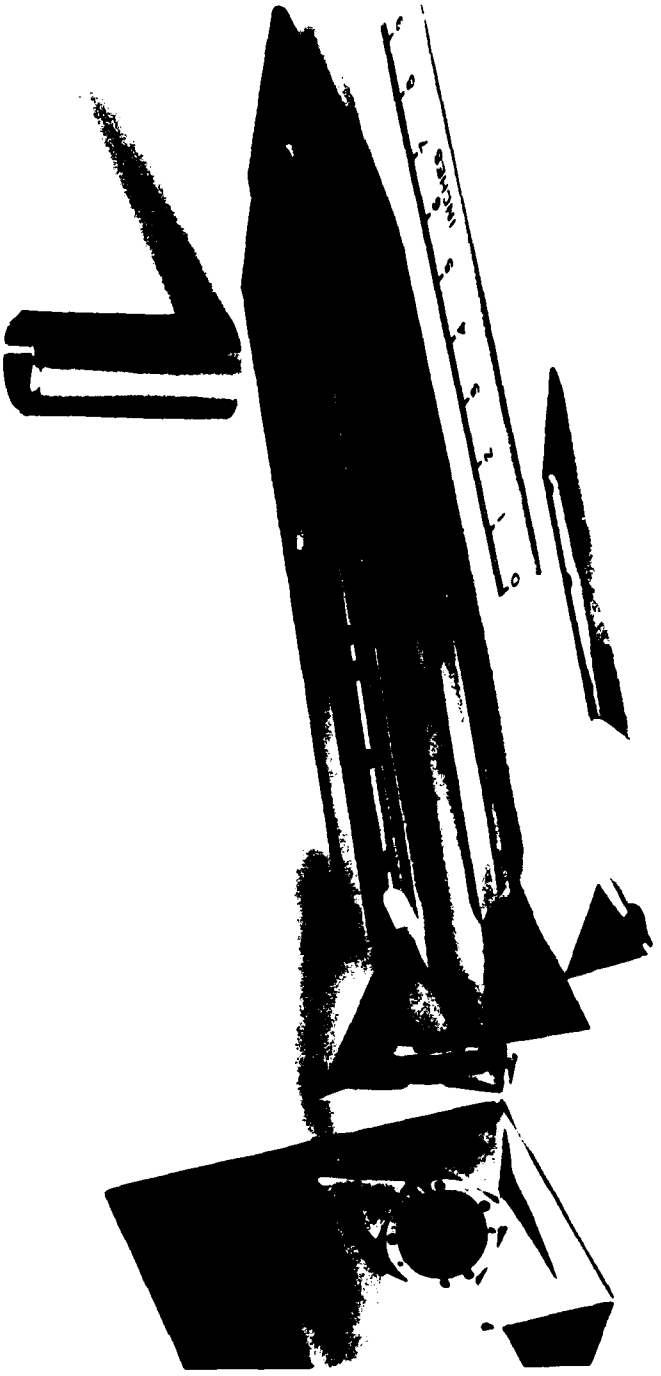

Fig. 2 Photo showing one type of very-low-aspect-ratio, thick wings used in analysis.

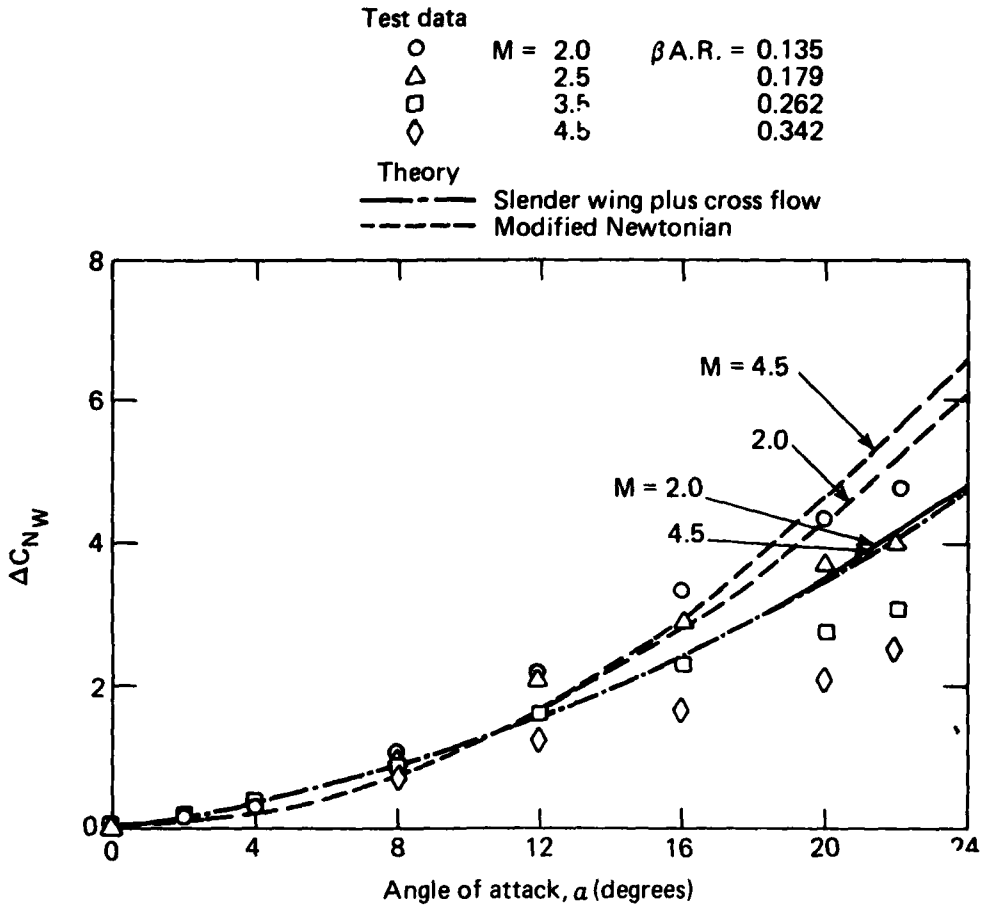

Fig. 3 Comparison of C_N data from IRR E_1 housing with two simple predictive methods $\phi = 0^o$.

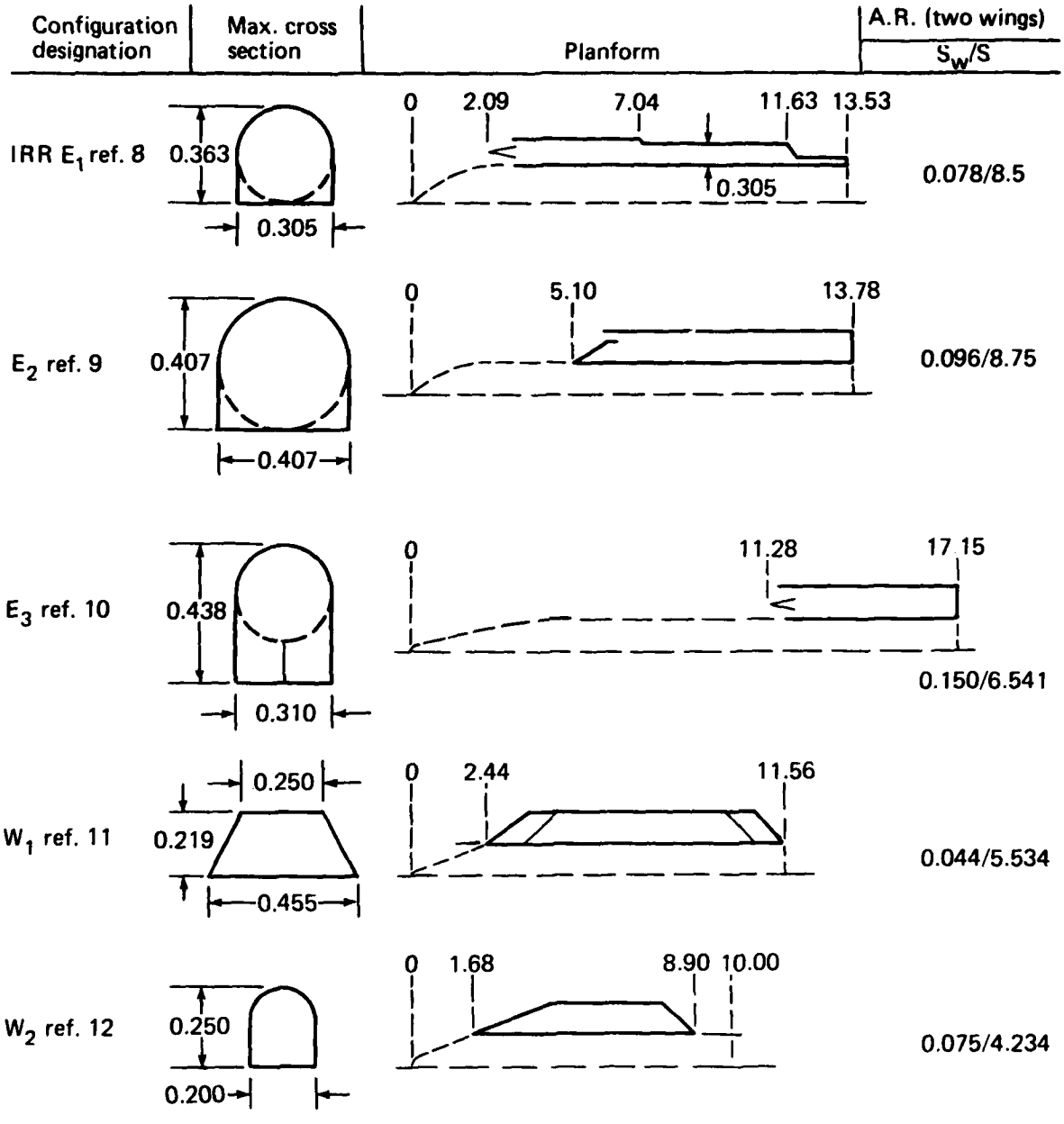

Fig. 4 Sketches of low A.R. wings (housings) used in analysis.

Ref. 13

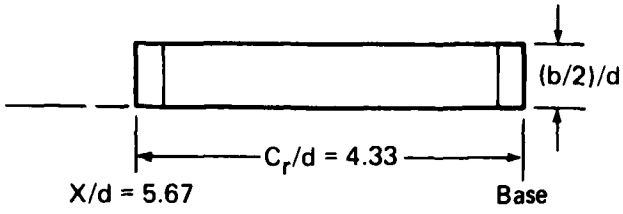

W_x	(b/2)/d	A.R. (two panels)	S_W/S
3	0.17	0.08	1.83
4	0.33	0.15	3.69
5	0.67	0.31	7.35

W_6 (ref. 14): A.R. = 0.120; S_W/S = 6.285

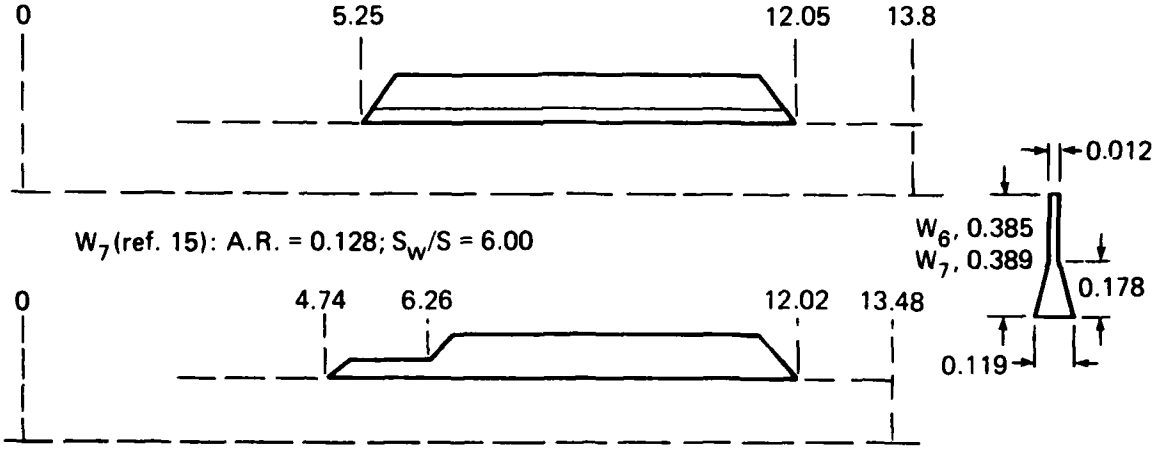

Dimensions in body diameters

Fig. 5 Thin, low-aspect-ratio, nearly-rectangular wings.

Ref. 13

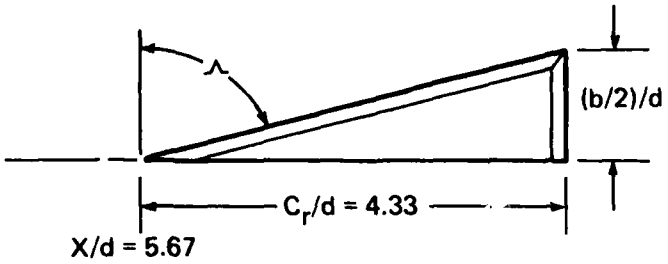

W_x	b/2/d	Λ	A.R. (two panels)	S_w/S
8	0.33	85.6°	0.31	1.83
9	0.67	81.3°	0.61	3.69
10	1.33	72.9°	1.23	7.35

Ref. 16

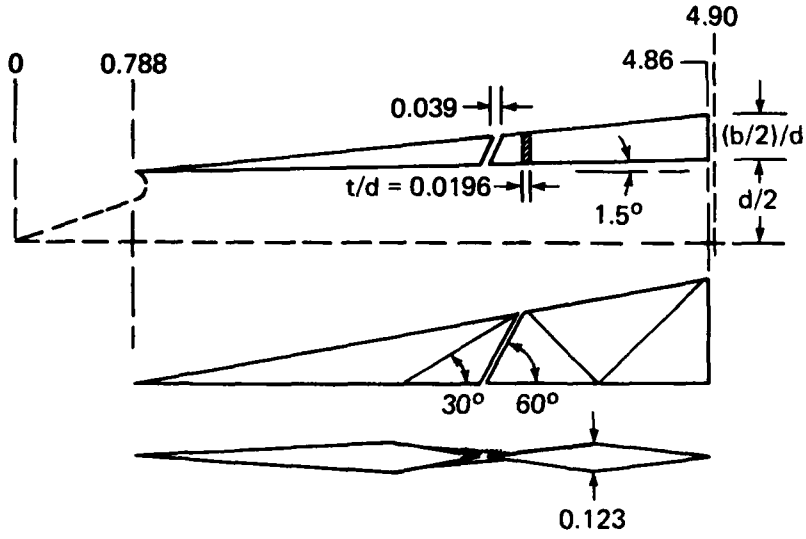

W_x	(b/2)/d	A.R.	S_w/S
11	0.088	0.088	0.453
12	0.206	0.204	1.057
13	0.706	0.710	3.61

Dimensions in body diameters

Fig. 6 Thin, low-aspect-ratio, delta wings.

Let ΔC_{N_W} be approximated, in range of α tested, by

$$\Delta C_{N_W} = C_{N_{\alpha_W}} (K_W + K_B)(S_W/S)\,\alpha/57.3$$

Then,

$$\beta C_{N_{\alpha_W}} = [\Delta C_{N_W}/\alpha](57.3\,\beta)/[(K_W + K_B)(S_W/S)]$$

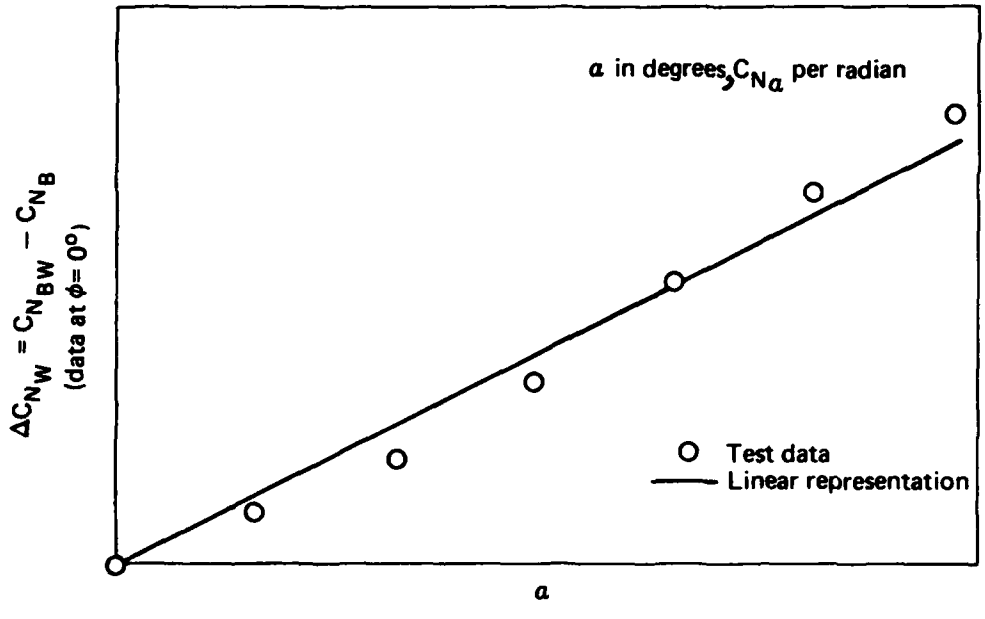

Fig. 7 Procedure used for linearization of test data to derive $\beta C_{N_{\alpha_W}}$

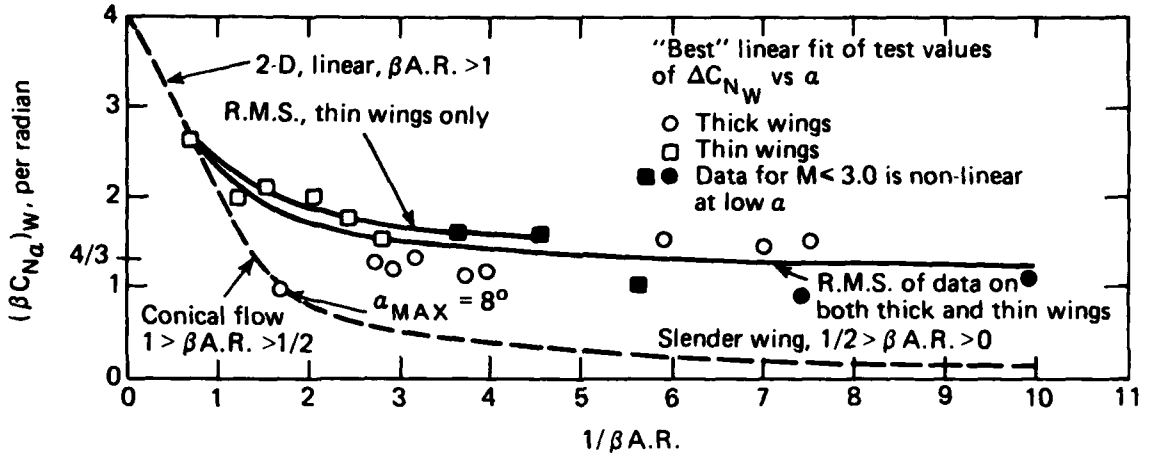

Fig. 8 Correlation of test data on nearly-rectangular wings with βA.R.

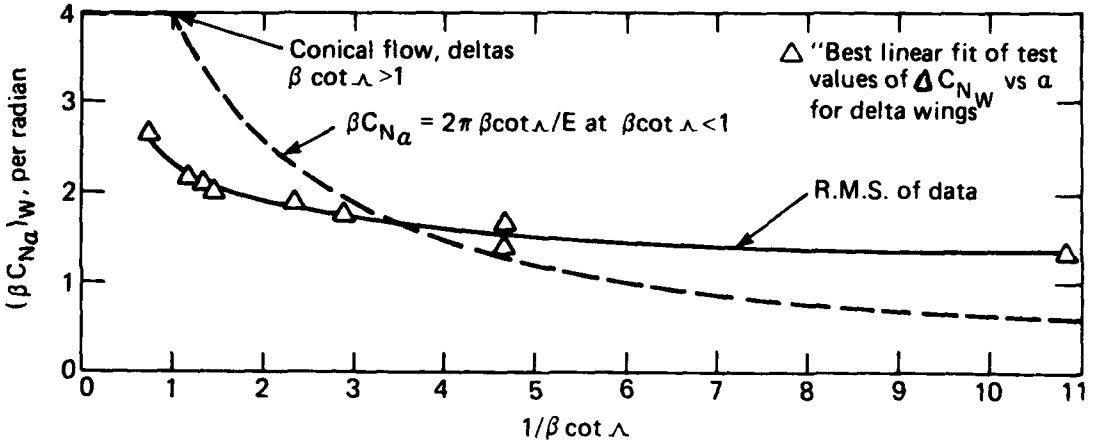

Fig. 9 Correlation of test data on thin delta wings with β cot Λ.

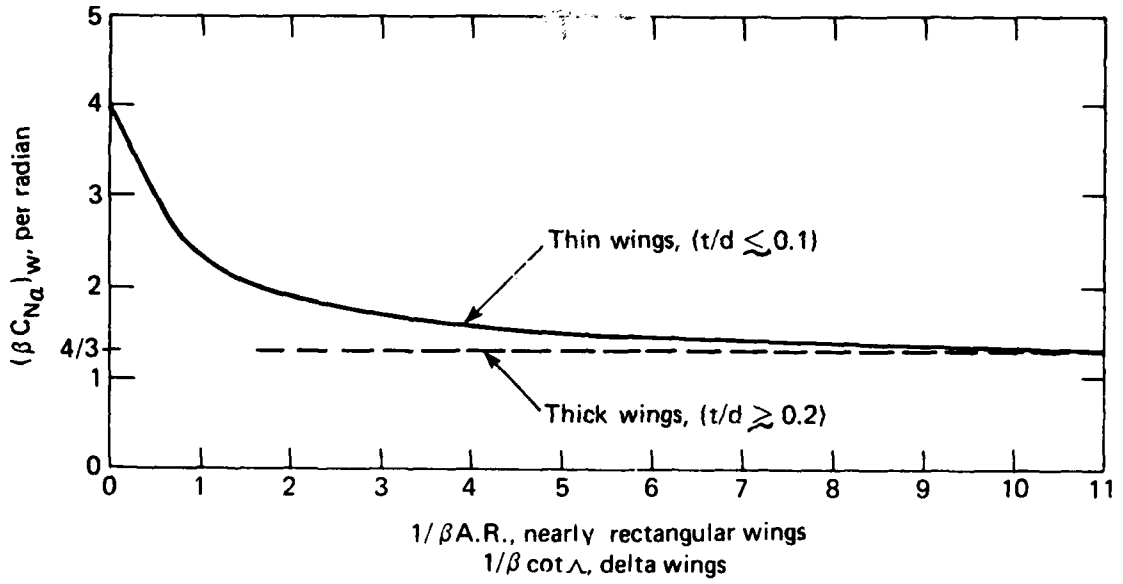

Fig. 10 Proposed design charts for βC_{N_α} of low-aspect-ratio wings M $\gtrsim$ 2.5 ϕ = 0°.

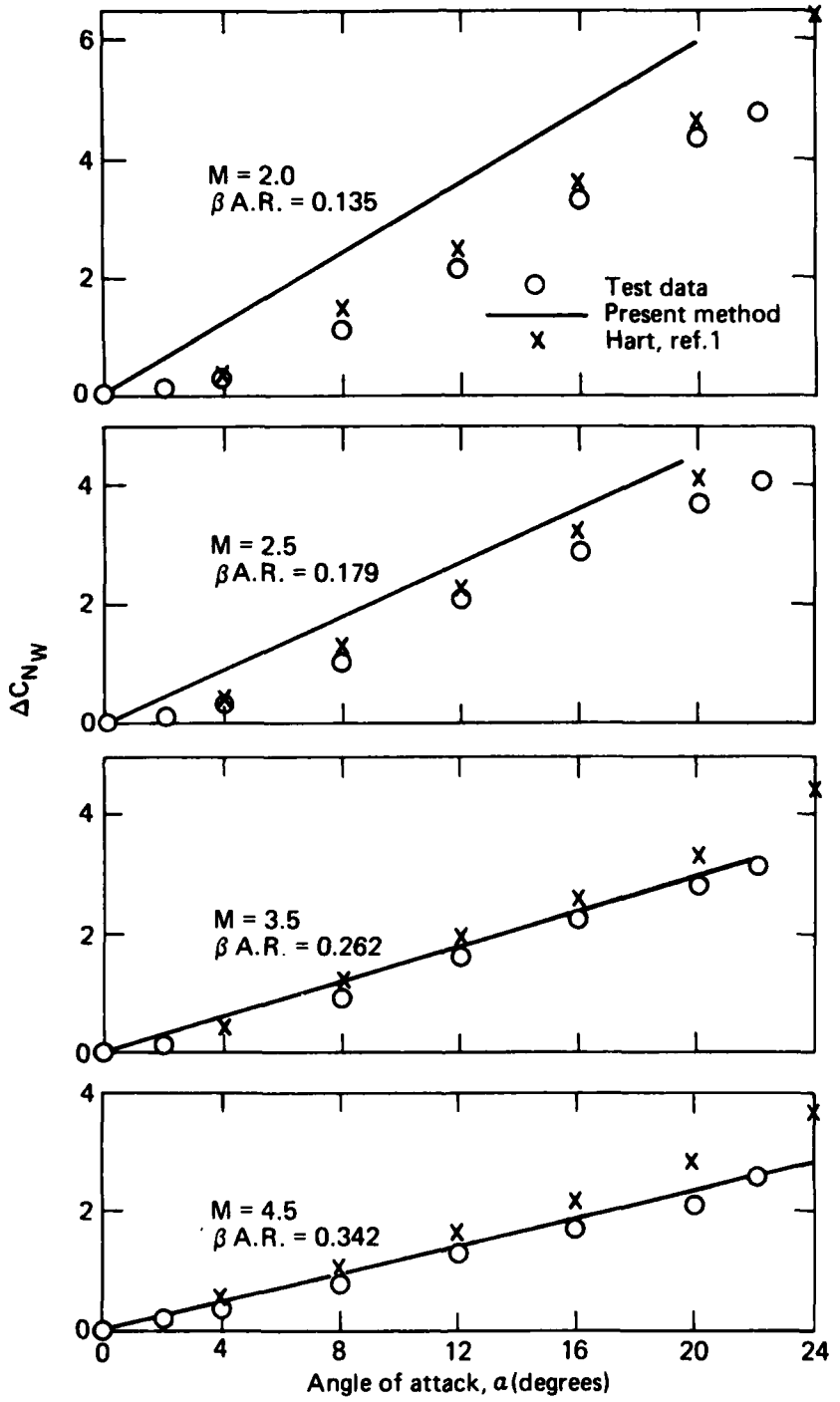

Fig. 11 Comparison of test and predicted values of ΔC_{N_W} of E_1, $\phi = 0°$, t/d = 0.305.

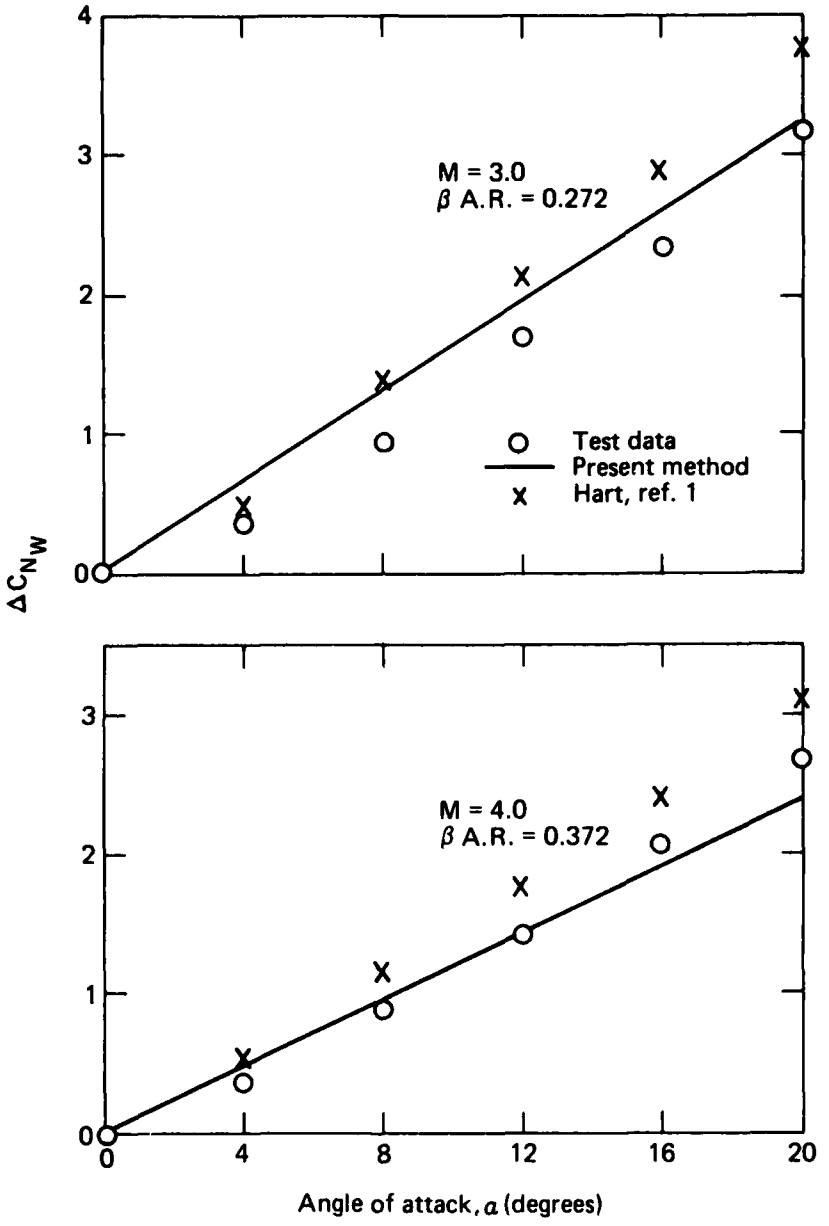

Fig. 12 Comparison of test and predicted values of ΔC_{N_W} of E_2, $\phi = 0°$, t/d = 0.407.

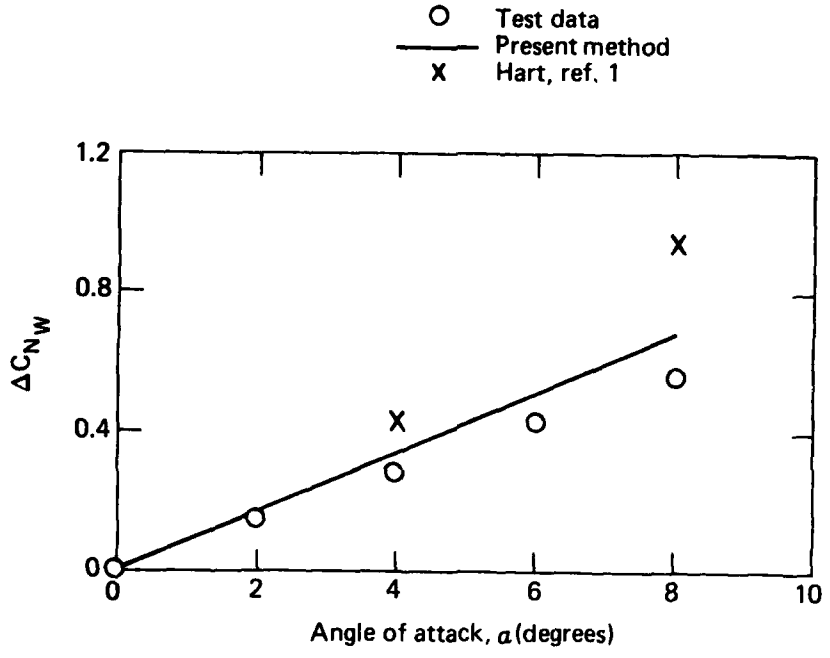

Fig. 13 Comparison of test and predicted values of ΔC_{N_W} of E_3, M = 4.17; ϕ = 0°, βA.R. = 0.607, t/d = 0.312.

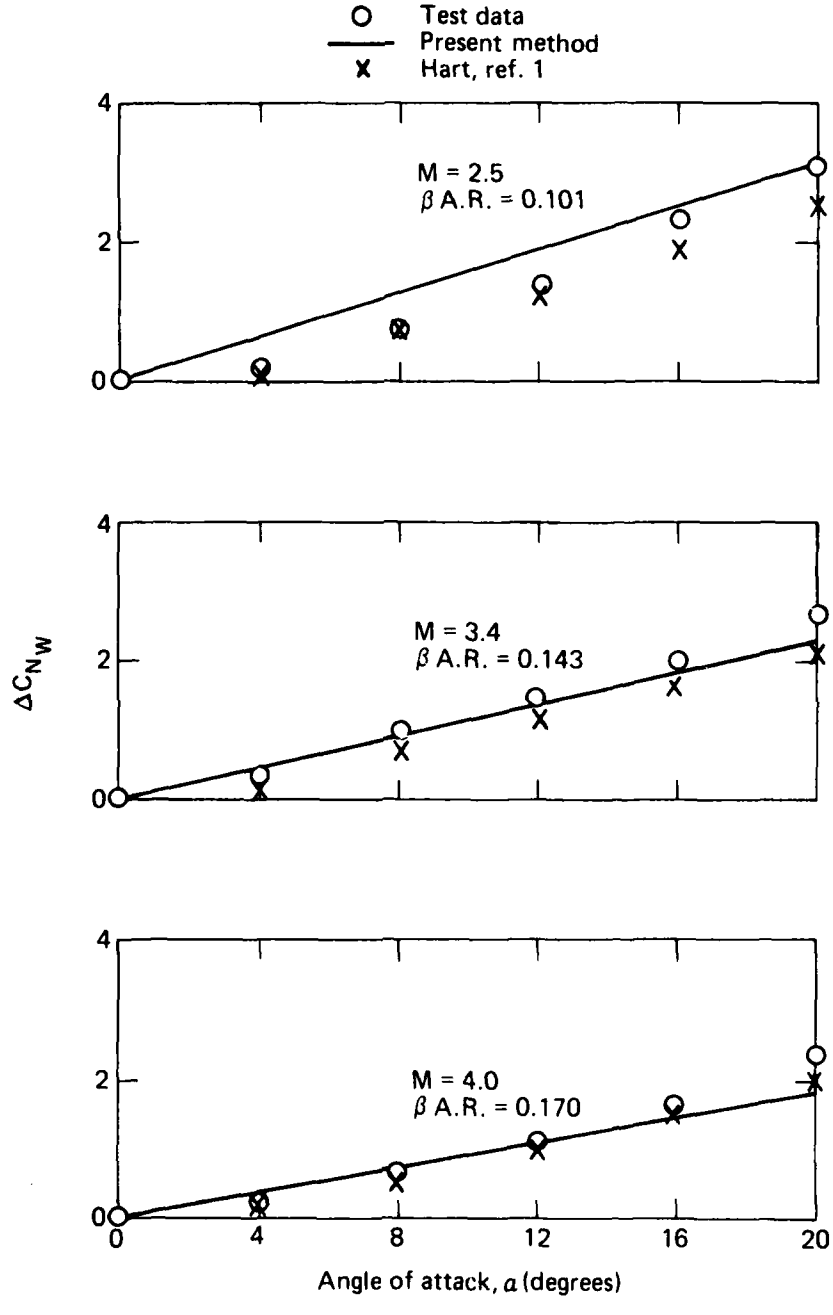

Fig. 14 Comparison of test and predicted values of ΔC_{N_W} of W_1, $\phi = 0°$, t/d = 0.352 Ave.

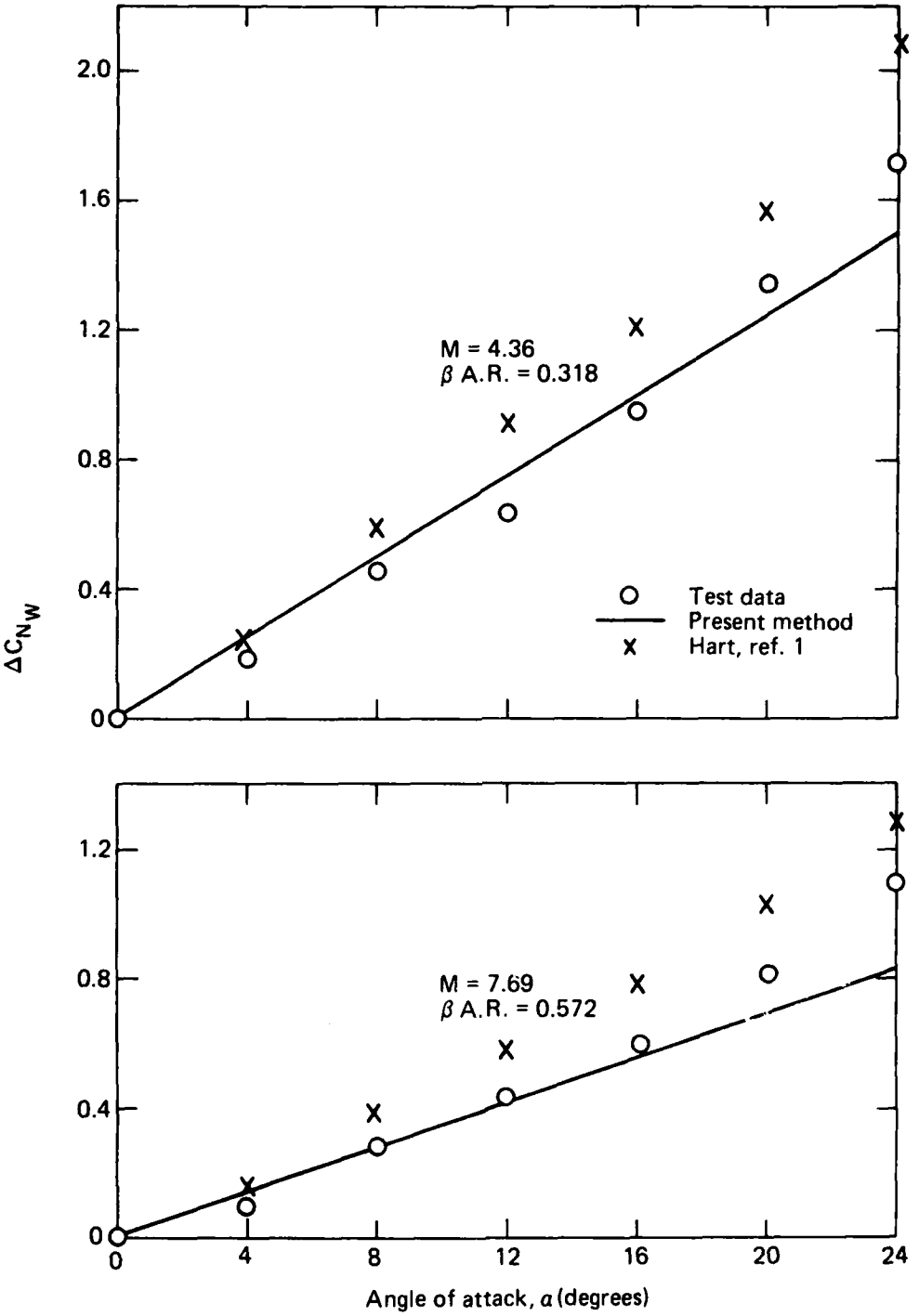

Fig. 15 Comparison of test and predicted values of ΔC_{N_W} of W_2, $\phi = 0°$, t/d = 0.200.

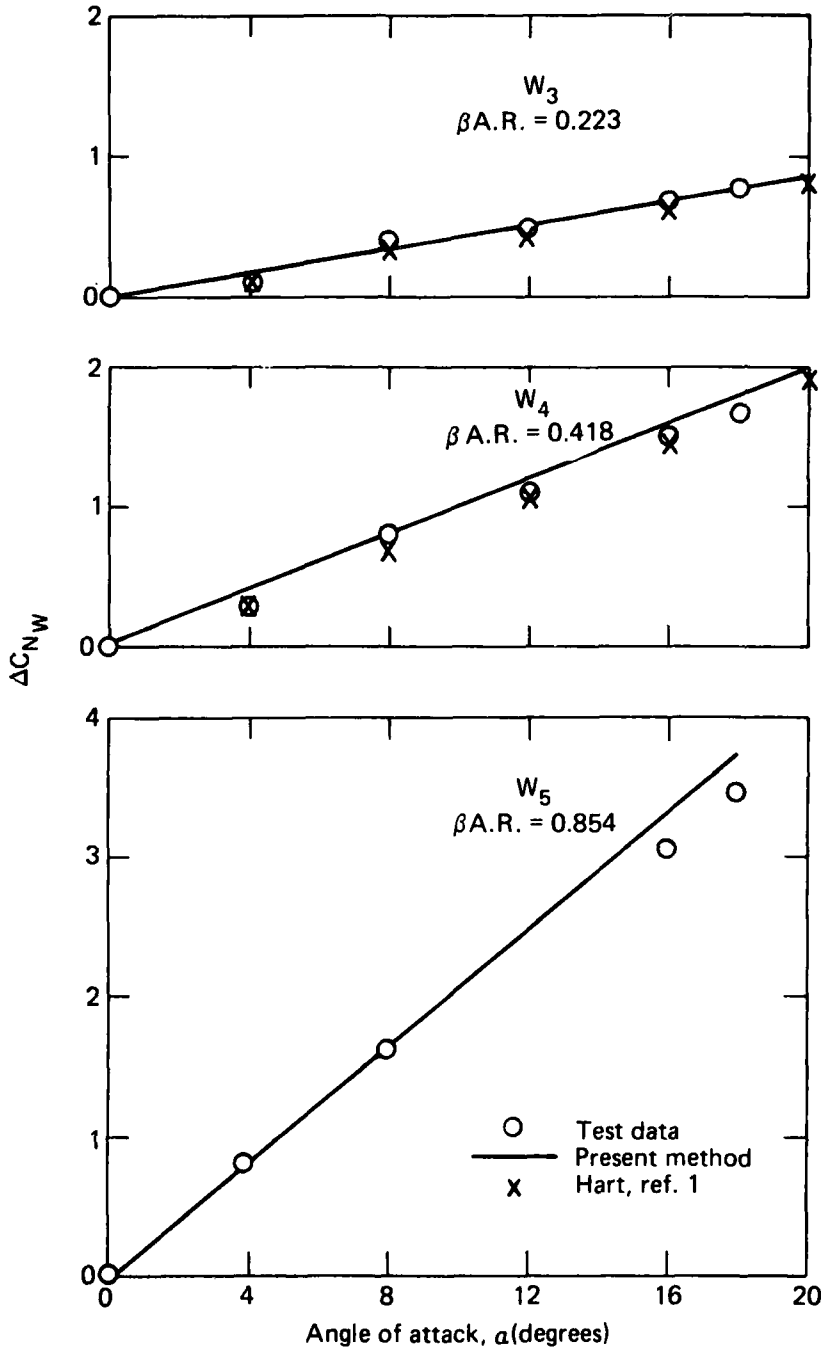

Fig. 16 Comparison of test and predicted values of ΔC_{N_W} for thin rectangular wings M = 2.96, $\phi = 0°$.

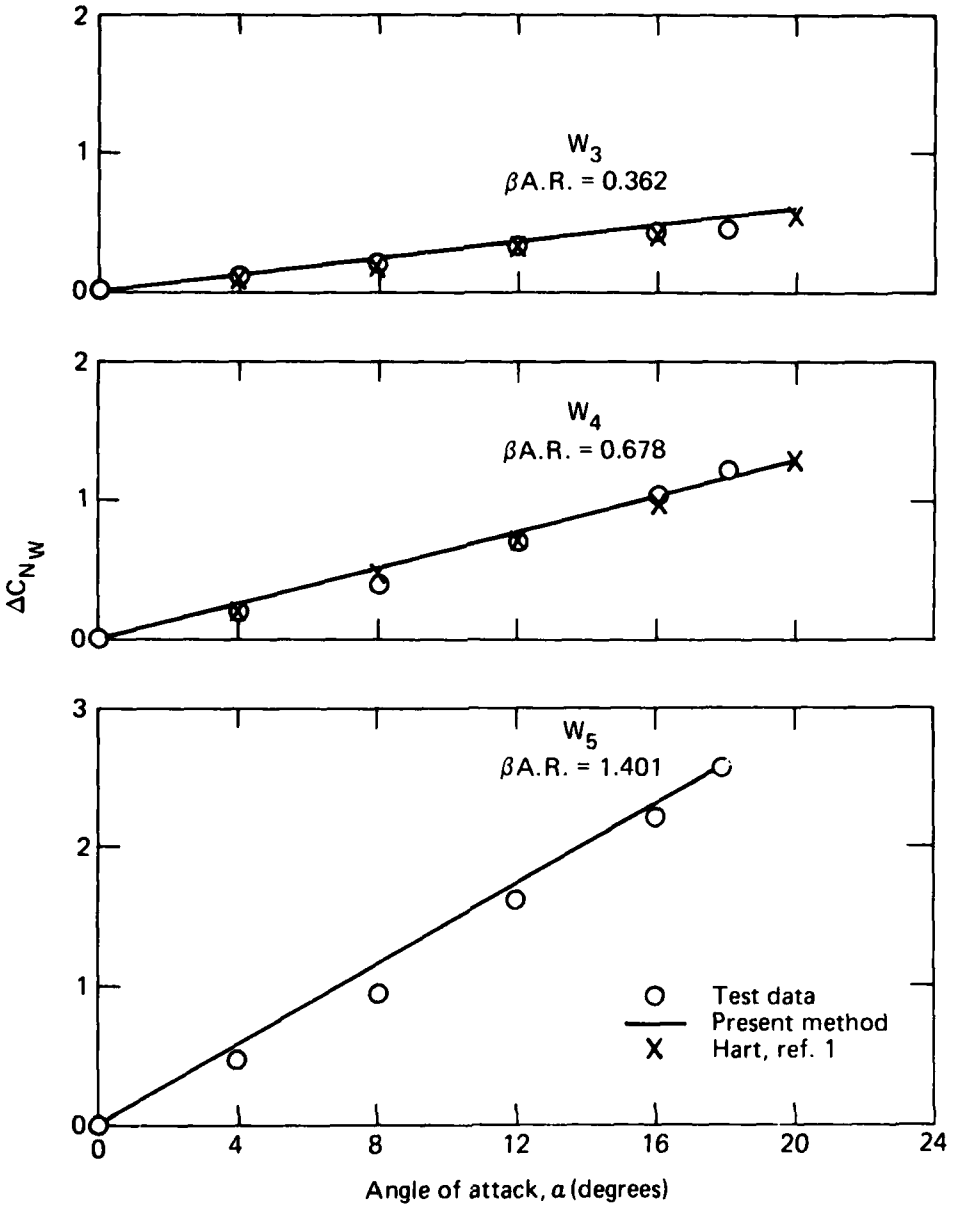

Fig. 17 Comparison of test and predicted values of ΔC_{N_W} for thin rectangular wings M = 4.63, ϕ = 0°.

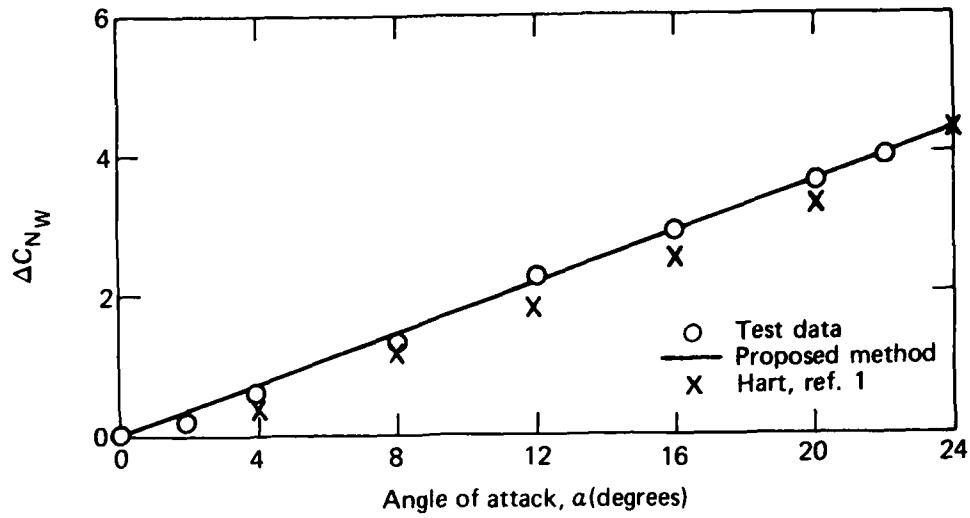

Fig. 18 Comparison of test and predicted values of ΔC_{N_W} for W_6, M = 2.5, ϕ = 0°, βA.R. = 0.275.

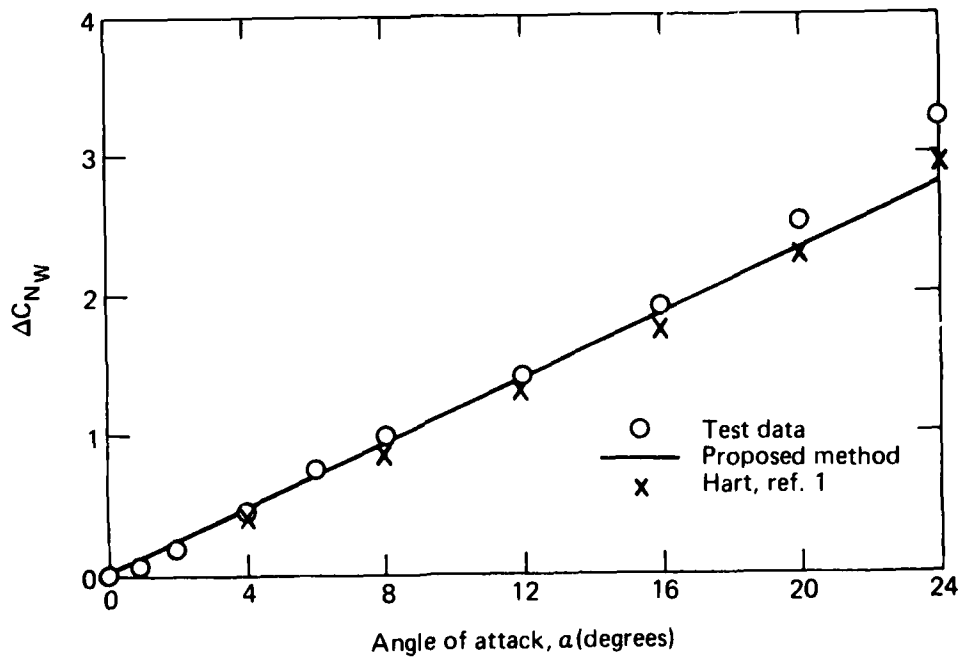

Fig. 19 Comparison of test and predicted values of ΔC_{N_W} for W_7, M = 4.02, ϕ = 0°, βA.R. = 0.498.

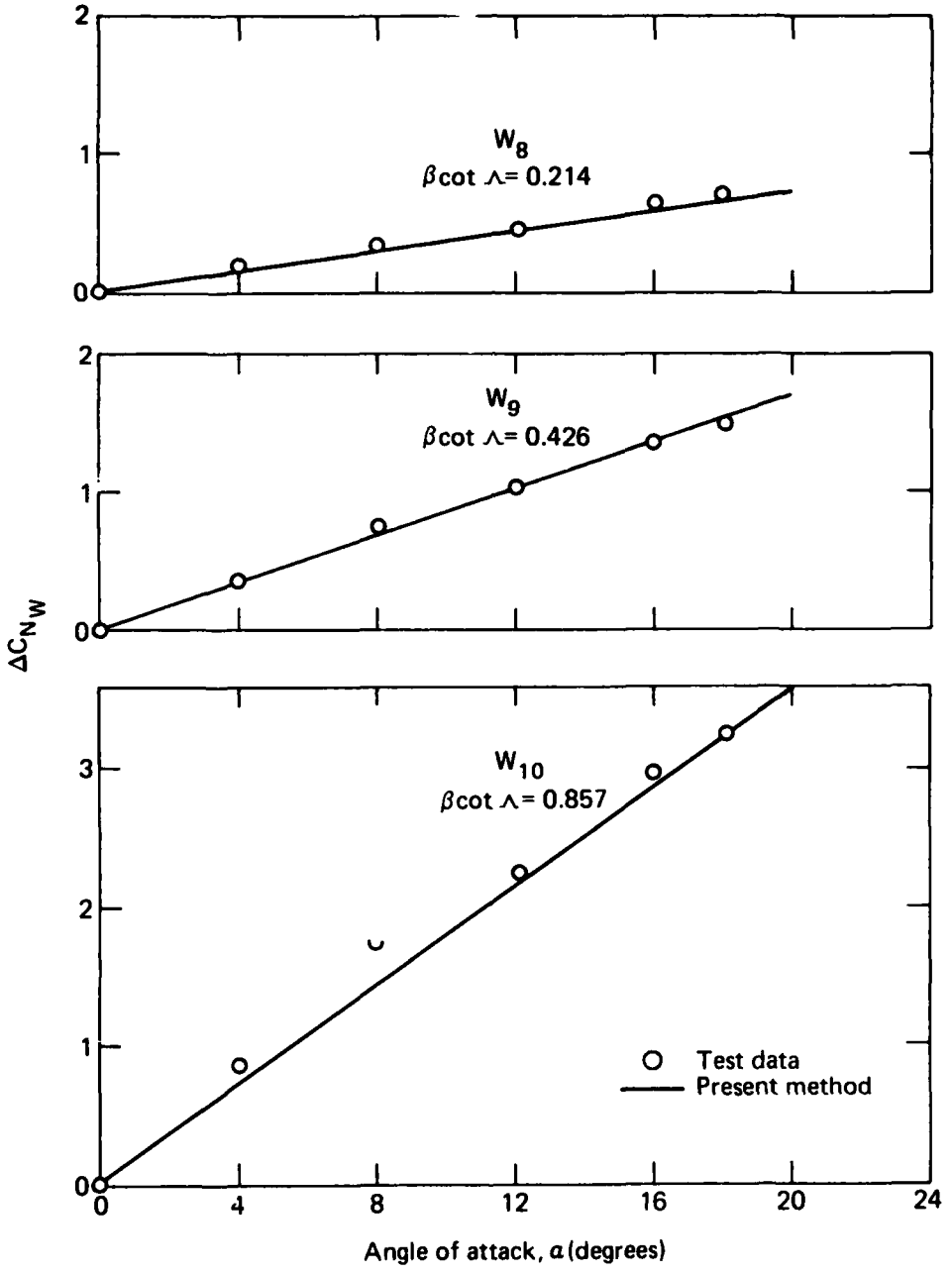

Fig. 20 Comparison of test and predicted values of ΔC_{N_W} for thin delta wings, M = 2.96, ϕ = 0°.

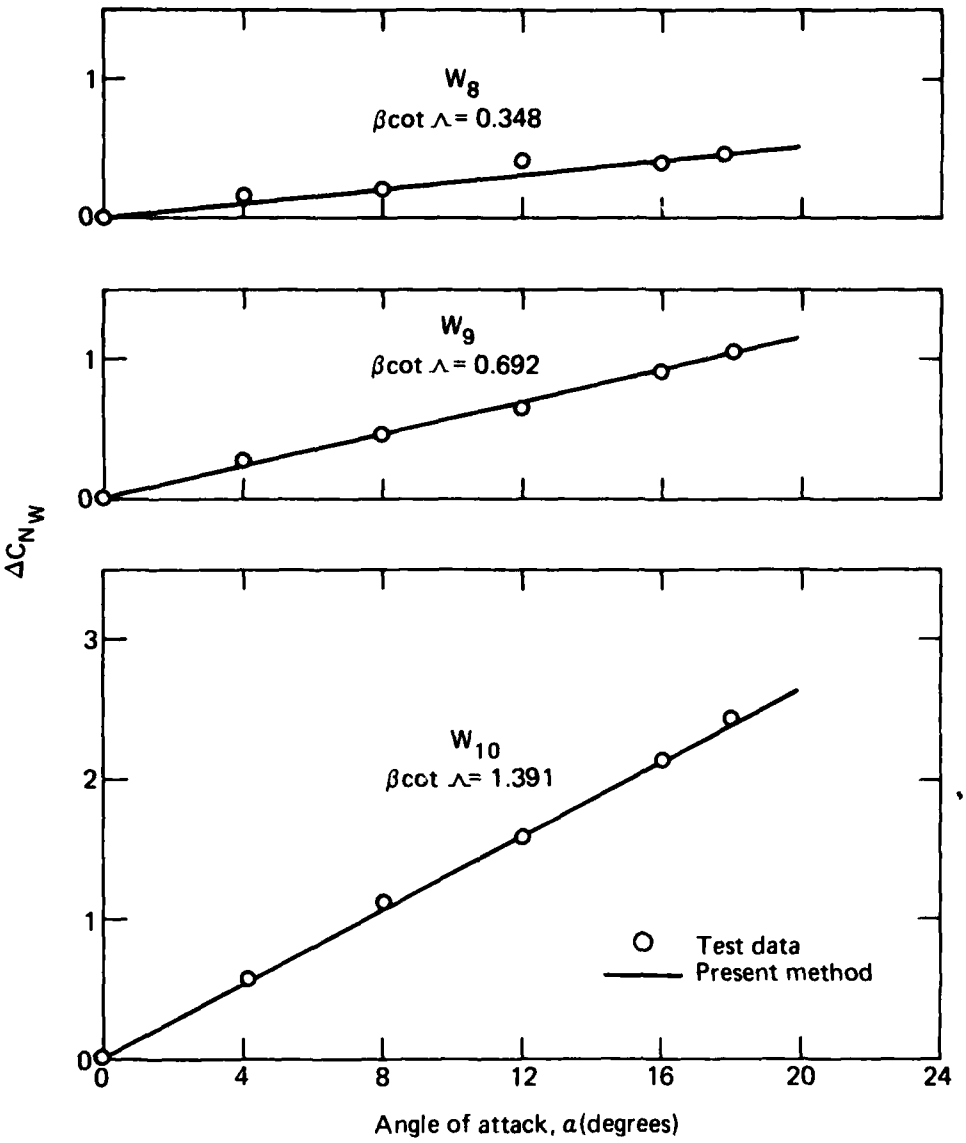

Fig. 21 Comparison of test and predicted values of ΔC_{N_W} for thin delta wings, M = 4.63, ϕ = 0°.

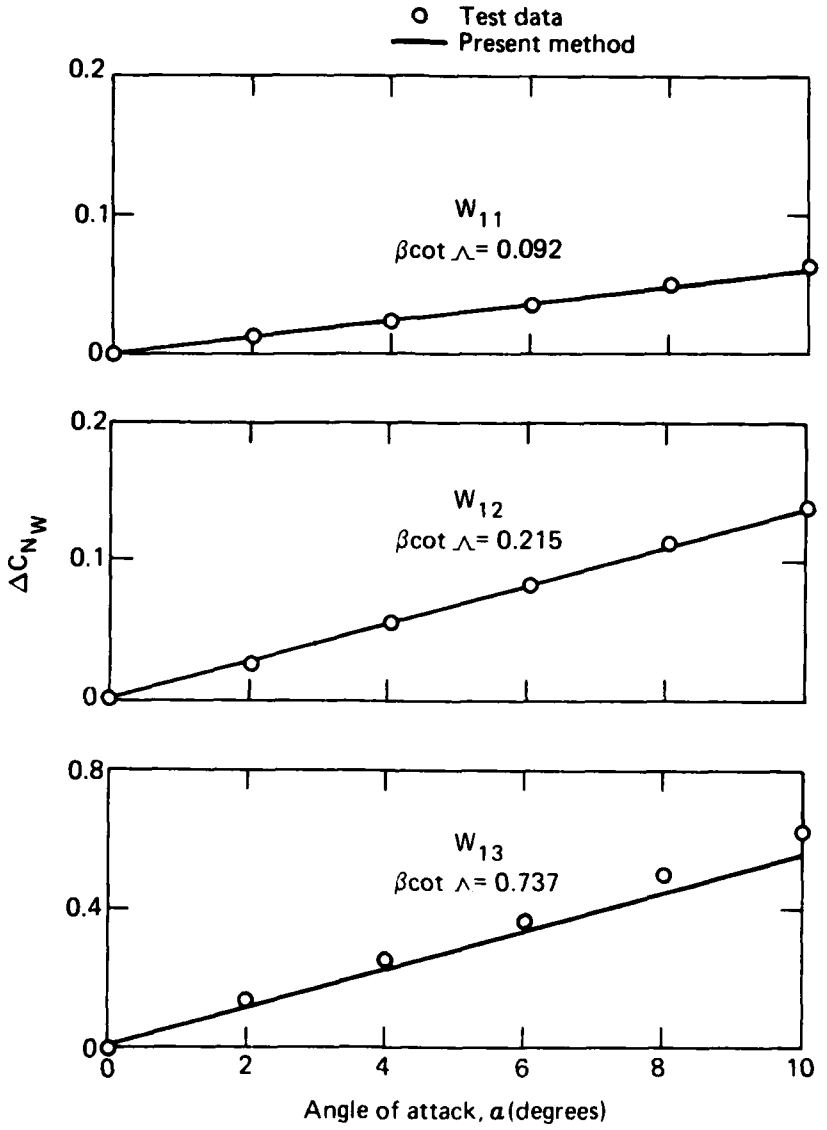

Fig. 22 Comparison of test and predicted values of ΔC_{N_W} of thin delta wings, M = 4.37, $\phi = 0°$.


DAT
FILM